TISSUE ENGINEERING: Part C
Volume 18, Number 1, 2012

DOI: 10.1089/ten.tec.2011.0339

An Osteochondral Culture Model to Study Mechanisms Involved in Articular Cartilage Repair

Marloes L. de Vries-van Melle, M.Sc.,[1] Erik W. Mandl, Ph.D.,[1,3] Nicole Kops, B.Sc.,[1] Wendy J.L.M. Koevoet, B.Sc.,[2] Jan A.N. Verhaar, M.D., Ph.D.,[1] and Gerjo J.V.M. van Osch, Ph.D.[1,2]

Although several treatments for cartilage repair have been developed and used in clinical practice the last 20 years, little is known about the mechanisms that are involved in the formation of repair tissue after these treatments. Often, these treatments result in the formation of fibrocartilaginous tissue rather than normal articular cartilage. Because the repair tissue is inferior to articular cartilage in terms of mechanical properties and zonal organization of the extracellular matrix, complaints of the patient may return. The biological and functional outcome of these treatments should thus be improved. For this purpose, an *in vitro* model allowing investigation of the involved repair mechanisms can be of great value. We present the development of such a model. We used bovine osteochondral biopsies and created a system in which cartilage defects of different depths can be studied. First, our biopsy model was characterized extensively: we studied the viability by means of lactate dehydrogenase (LDH) excretion over time and we investigated expression of cartilage-related genes in osteochondral biopsies and compared it with conventional cartilage-only explants. After 28 days of culture, LDH was detected at low levels and mRNA could be retrieved. The expression of cartilage-related genes decreased over time. This was more evident in cartilage-only explants, indicating that the biopsy model provided a more stable environment. We also characterized the subchondral bone: osteoclasts and osteoblasts were active after 28 days of culture, which was indicated by tartrate acid phosphatase staining and alkaline phosphatase measurements, respectively, and matrix deposition during culture was visualized using calcein labeling. Second, the applicability of the model was further studied by testing two distinct settings: (1) implantation of chondrocytes in defects of different depths; (2) two different seeding strategies of chondrocytes. Differences were observed in terms of volume and integration of newly formed tissue in both settings, suggesting that our model can be used to model distinct conditions or even to mimic clinical treatments. After extensive characterization and testing of our model, we present a representative and reproducible *in vitro* model that can be used to evaluate new cartilage repair treatments and study mechanisms in a controlled and standardized environment.

Introduction

Due to the low intrinsic repair capacity of cartilage, untreated cartilage lesions are destined to progress into early osteoarthritis (OA). Several treatment options have been developed over the last 20 years, including autologous chondrocyte implantation (ACI). In ACI, cartilage is harvested arthroscopically from nonweight-bearing areas of the joint and digested to isolate chondrocytes, which are expanded in culture. After obtaining a sufficient number, the cells are implanted back into the joint, covered by a periosteal flap.[1] Over the years, several variations of this treatment have been investigated and introduced, including the use of biomaterials to cover the defect or to seed the chondrocytes on before implantation.[2,3]

Other examples of treatments for cartilage lesions are marrow stimulation techniques, such as the microfracture procedure popularized by Steadman. In this single-surgery procedure, conical holes are punched through the subchondral plate, allowing a bone marrow clot to fill the defect.[4,5] The formation of repair tissue is addressed to mesenchymal stem cell (MSC) differentiation and possibly migration of cells from the surroundings into the defect.[6]

For both ACI-based treatments and the microfracture procedure, the formed repair tissue is often of fibrocartilaginous nature, which does not have the desired zonal organization of the extracellular matrix (ECM) nor mechanical properties similar to those of the native articular cartilage. Also, return of complaints is often reported from 24 months posttreatment.[7–9]

Current articular cartilage repair strategies require improvement in terms of biological and functional outcome, which would either be achieved by improving current treatments or developing new cartilage repair strategies.[10,11]

Departments of [1]Orthopaedics and [2]Otorhinolaryngology, Erasmus MC, University Medical Centre Rotterdam, The Netherlands.
[3]Department of Orthopaedics, Albert Schweitzer Hospital, Dordrecht, The Netherlands.

To achieve this, insight is required in the working mechanisms behind the existing treatments. Knowledge on several topics involved in the repair process could provide these insights: identification of the optimal cell source, integration of formed repair tissue into the native tissue, and the role of cells present in the native tissue. For example, removal of the calcified cartilage without damaging the subchondral plate is reported as critical step in the microfracture procedure, while the exact mechanistic reason for this step being critical is unknown.[12] Altogether, the basic repair mechanisms involved in current treatments are still largely unknown.[7,13,14] To improve biological and functional outcome or even to prevent the development and progression of early OA, these mechanisms need to be elucidated. To study these mechanisms, we developed a model that can provide more complexity than cell culture, and less complexity and more standardization than animal models.

In this study, we present the development and testing of an osteochondral culture model. We first evaluated cartilage and bone metabolism over time in culture, particularly focusing on cartilage metabolism in osteochondral biopsies compared with the cartilage-only explant system that is regularly used. Then we demonstrated that defect depth can be controlled reproducibly, and finally, we tested the applicability of our model to study cell-based cartilage repair strategies *in vitro* by seeding cells in created defects. We conclude that this multifunctional osteochondral culture model can be used to evaluate new methods to repair cartilage and to study the mechanisms involved in articular cartilage repair.

Materials and Methods

Osteochondral biopsy obtainment and culture

The four proximal sesamoïd bones of fresh metacarpal-phalangeal (MCP) joints from 3- to 8-month-old calves were used to create osteochondral biopsies using a 8 mm diameter diamond-coated trephine drill (Synthes). Per MCP joint, four biopsies were obtained. Subsequently, biopsies were washed in Dulbecco's modified Eagle's medium-high glucose (4.5 g/L glucose; Gibco) supplemented with 10% fetal bovine serum (Lonza), 50 μg/mL gentamicine (Gibco), and 1.5 μg/mL fungizone (Gibco), from now on referred to as "culture medium." Biopsies were cut to about 5 mm in length and kept overnight in culture medium to verify sterility. Biopsies were placed in a 2% low-gelling agarose (gelling temperature 37–39°C; Eurogentec) in physiological saline solution, such that the subchondral bone was surrounded by agarose and the cartilage was above the agarose surface to prevent outgrowth of cells from the subchondral bone. For comparison, cartilage explants without bone were obtained from fresh bovine MCP joints using a 6 mm diameter dermal biopsy punch (Stiefel Laboratories) and scalpel. Unless stated otherwise, all osteochondral biopsies and cartilage explants were cultured for 28 days in culture medium at 37°C and 5% CO_2. Medium was refreshed three times per week.

Characterization of the model: viability and activity

Osteochondral biopsy viability and bone-matrix activity were studied. Lactate dehydrogenase (LDH), which was excreted by dying cells, was measured in medium at every refreshment as nondestructive method to indicate cell death during culture. Alkaline phosphatase (ALP) activity was measured in medium at every refreshment as a measure for bone formation activity. Medium was divided into two portions, one of which was subjected to LDH assay immediately and the other was stored at −80°C for ALP assay.

The LDH assay (Roche Diagnostics) was performed according to the manufacturer's instructions. In short, 100 μL used culture medium was incubated for 30 min in the dark with 100 μL reagents consisting of 98% dye solution and 2% catalyst. Culture medium that was not used for culture was used for blank measurement. Absorbance was measured at 490 nm using a Wallac 1420 victor2 spectrophotometer (Perkin-Elmer).

ALP activity was measured in medium by determining the release of paranitrophenol as described previously.[15] In short, medium was incubated for 10 min at 37°C with 20 mM paranitrophenylphosphate in 1M diethanolamine buffer supplemented with 1 mM $MgCl_2$ at pH 9.8. Subsequently, the reaction was stopped by adding 0.06 M NaOH. Adsorption was measured at 405 nm using a Wallac 1420 victor2 spectrophotometer (Perkin-Elmer).

To study the effect of culturing on bone and cartilage in our osteochondral model, osteochondral biopsies and cartilage explants were harvested directly after preparation, after 7 and 28 days of culture for RNA isolation and quantitative polymerase chain reaction (qPCR). Cartilage explants were snap-frozen in liquid nitrogen. For the osteochondral biopsies, cartilage and bone were separated using a scalpel and separately snap-frozen in liquid nitrogen. All samples were stored at −80°C until further processing. To evaluate tissue morphology and to assess osteoclast activity, osteochondral biopsies were fixed in 4% formalin for at least 24 h and subsequently processed for histology as described in the histology section.

Characterization of the model: matrix deposition

To study bone-matrix deposition, biopsies with osteochondral defects were labeled overnight after 14 days of culture to verify matrix deposition during culture using 2 mg/mL calcein (Sigma-Aldrich) suspended in medium supplemented with 2 mg/mL sodium carbonate. To allow matrix deposition, culture medium was supplemented with 0.1 μM dexamethasone (Sigma-Aldrich) and 10 mM β-glycerol phosphate (Sigma-Aldrich). Calcein-labeled biopsies were harvested for fluorescence microscopy and histology directly after overnight labeling and 14 days after labeling. Samples were fixed in 4% formalin for at least 24 h and subsequently processed for methylmethacrylate (MMA) embedding as described in the histology section.

Testing the applicability of the model for studying cell-based treatments

To validate the osteochondral culture model, two settings were tested: (1) seeding of chondrocytes in defects of three different depths: shallow cartilage defects, full-thickness cartilage defects, and osteochondral defects; (2) applying two different seeding strategies in osteochondral defects: direct seeding of chondrocytes versus chondrocytes seeded on membranes before placement in the defect.

To evaluate the feasibility of creating a model to study the effect of different depths of defects in the osteochondral biopsies, we used a 6 mm diameter dermal biopsy punch (Stiefel Laboratories) and scalpel to create one defect per biopsy of chondral (shallow, Fig. 1A), subchondral (intermediate, Fig. 1B), or osteochondral (deep, Fig. 1C) nature. Defect depth was controlled by the extent of removal of tissue. To obtain chondral defects, a thin layer of cartilage was removed carefully. For subchondral defects, cartilage was removed down to the calcified cartilage layer, which remained intact. To obtain osteochondral defects, the calcified cartilage layer was removed and parts of the subchondral bone were removed by scraping the surface using a scalpel. To investigate the effect of defects of different depths on repair by seeded cells, bovine chondrocytes were isolated from cartilage explants from MCP joints. Explants were incubated for 90 min in physiological saline supplemented with 0.2% protease (Sigma-Aldrich). Subsequently, explants were digested overnight in culture medium supplemented with 0.15% collagenase B (Roche Diagnostics). The cell suspension was filtered and washed in physiological saline. Cell numbers were determined using a hemocytometer. P0 bovine chondrocytes were seeded into the defects of different depths at a concentration of 4×10^6 cells per defect in 100 µL culture medium, incubated for 1 h at 37°C, centrifuged at 1300 rpm for 30 s, and subsequently covered with a 5 mm diameter ChondroGide membrane (Geistlich Biomaterials) and sealed with TissueCol fibrin glue (Baxter; Fig. 1E.1). Biopsies were harvested for histology after 28 days of culture.

To test a second setting, defects of osteochondral depth were created as described. Bovine chondrocytes were either seeded into the defects as described above or seeded onto a 5 mm diameter ChondroGide membrane at a density of 4×10^6 cells per membrane, precultured for 3 days, and subsequently placed in osteochondral defects and sealed with TissueCol fibrin glue (Fig. 1E.2). Biopsies were harvested for histology after 28 days of culture.

Histology

Upon harvesting for histology, biopsies were fixed in 4% formalin for at least 24 h. Biopsies were either embedded in MMA, or decalcified in 10% formic acid in PBS and embedded in paraffin, and sectioned in 5 µm sections. For staining of MMA sections, slides were deplastified by incubation in a 1:1 mixture of xylene and chloroform for 60 min and subsequently hydrated. For staining of paraffin sections, slides were deparaffinized using xylene and subsequently hydrated.

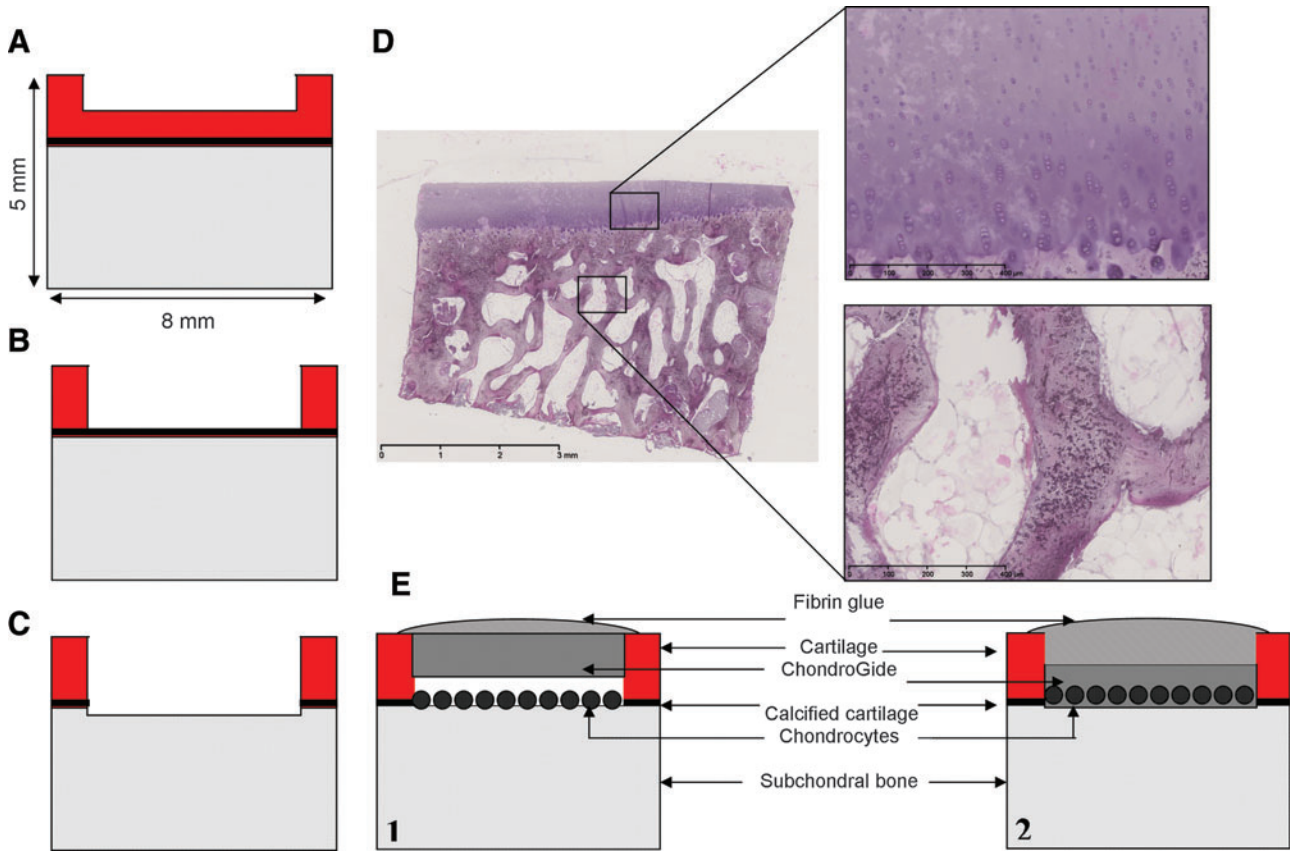

FIG. 1. **(A)** Schematic representation of the biopsy model with a chondral defect, **(B)** with a subchondral defect, **(C)** with an osteochondral defect, **(D)** H&E-stained osteochondral biopsy after 28 days of culture; scale bar indicates 3 mm. Insets: detail images of cartilage and bone, respectively, scale bars indicate 400 µm. **(E)** Schematic representation of validation settings of the osteochondral biopsy model: (1) osteochondral defect seeded with bovine chondrocytes covered with a ChondroGide membrane and fibrin glue; (2) osteochondral defect with a ChondroGide membrane, preseeded with bovine chondrocytes covered with fibrin glue. H&E, hematoxylin and eosin. Color images available online at www.liebertonline.com/tec

Hematoxylin and eosin (H&E) staining was performed to study general cell morphology and safranin-O staining was performed to visualize glycosaminoglycans in the ECM. Stainings were performed on MMA or paraffin sections. For safranin-O staining, slides were first stained with 0.1% light green in distilled water for 5 min, subsequently washed in 1% acetic acid and stained with 0.1% safranin-O (Fluka).

MMA sections were stained using tartrate resistant acid phosphatase (TRAP) to verify osteoclast activity as described previously.[16,17] In short, slides were incubated for 20 min in 0.2 M acetate buffer containing 50 mM L(+)tartaric acid (Acros Organics), whose pH was set at 5. Slides were then incubated in 0.2 M acetate buffer containing 0.5 mg/mL naphtol AS-MX phosphate (Sigma-Aldrich) and 1.1 mg/mL fast red TR salt (Sigma-Aldrich) for 1–4 h, during which the progress of the staining was monitored. Slides were counterstained with hematoxylin.

Quantification of repair tissue

In the experiments performed to test the applicability of the osteochondral culture model for studying cartilage repair mechanisms *in vitro*, repair tissue formed by seeded chondrocytes was defined as safranin-O positive-stained tissue other than the native cartilage, which was visually discriminated. We used ImageJ software to score both the extent of newly formed repair tissue attached to or directly lying alongside the bottom of the created cartilage defects and the volume of the newly formed repair tissue. Volume of repair tissue was defined as the amount of mm^2 safranin-O–positive repair tissue; integration was defined as percentage of the bottom of the defect covered with safranin-O–positive repair tissue. Three sections were scored per biopsy.

RNA isolation and qPCR

Deep-frozen samples were pulverized at 1,000 rpm using a Mikro-Dismembrator S (B. Braun Biotech International GmbH). Pulverized samples were rapidly covered with 1.8 mL/g RNABee (TEL-TEST). Chloroform was added at a quantity of 200 µL per mL RNABee. Further RNA isolation was performed using the RNeasy Microkit (Qiagen) according to manufacturer's instructions, including on-column DNAse treatment. RNA concentration and quality was measured using a spectrophotometer (NanoDrop ND1000 UV-VIS, Isogen Life Science B.V.). cDNA was prepared using RevertAid First Strand cDNA Synthesis Kit (MBI Fermentas) according to manufacturer's instructions. qPCR was performed in 20 µL reactions on an ABPrism 7000 system (Applied Biosystems) using either TaqMan Universal PCR mastermix (Applied Biosystems) or SybrGreen (Eurogentec). Expression of collagen type 2 (Fw: CCGGTATGTTTCGTG CAGCCATCCT; Rv: GGCAATAGCAGGTTCACGTACA),[18] collagen type 1 (Fw: CAGCCGCTTCACCTACAGC; Rv: TTTTGTATTCAATCACTGTCTTGCC; probe: Fam-CGGTG TGACTCGTGCAGCCATC-Tamra), aggrecan (Fw: AATTAC CAGCTACCCTTCACCTGTA; Rv: TCCGAAGATTCTGGC ATGCT),[18] collagen type X (Fw: ACTTCTCTTACCACAT ACACG; Rv: CCAGGTAGCCCTTGATGTACT), matrix metalloproteinase 13 (MMP13, Fw: TCTTGTTGCTGCCCATG AGT; Rv: GGCTTTTGCCAGTGTAGGTGTA),[18] and of the aggrecanases a disintegrin and metalloproteinase with thrombospondin motifs 4 (*ADAMTS4*) (Fw: GAAGCAAT GCACTGGTC TGA; Rv: CCGAAGCCATTGTCTAGGAA) and *ADAMTS5* (Fw: GCAGTATGACAAATGTGGCG; Rv: TTTATGTGAGT CGCCCCTTC) was assessed. Glyceraldehyde-3-phosphate dehydrogenase (GAPDH, Fw: GTCAACGGATTT GGTCG TATTGGG; Rv: TGCCATGGGTGGAATCATATTGG; probe: Fam-TGGCGCCCCAACCAGCC-Tamra)[19] and β-Actin (Fw: TTACAACGAGCTGCGTGTGG; Rv: TGGCAGGAGTG TT GAACGTC) were tested as reference genes. Relative gene expression was calculated using the $2^{-\Delta CT}$ method.[20]

Statistics

The results of histological scoring and of qPCR data were statistically tested using the Student's *t*-test. Differences were considered statistically significant for $p < 0.05$.

Results

Characterization of the model

To verify the viability of the cells present in the osteochondral biopsies, LDH, which was secreted by dying cells, was measured in the culture medium three times per week. LDH secretion of osteochondral biopsies was compared with that of cartilage-only explants (Fig. 2A). As was expected, during the first day in culture, relatively high levels of LDH—caused by explantation and drilling of the tissue—were measured. From day 7, the LDH levels were much lower and became relatively stable for the remaining days of culture. In the cartilage-only explants, overall lower amounts of LDH were observed indicating less dying cells, which can be explained by the fact that less cells were present in the cartilage-only explants than in the osteochondral biopsies.

TRAP-stained active osteoclasts were found in both biopsies harvested directly after isolation and biopsies cultured for 28 days, which indicated that the bone was still actively remodeling after 28 days of culture (Fig. 2C). As an indication of osteoblast activity, ALP activity was initially high, decreasing to a relatively stable level after 1 week of culture (Fig. 2B). Calcein labeling showed that bone matrix was deposited during culture, visualized as green staining covered by matrix deposited after labeling, which is another indication for active remodeling of the bone during culture (Fig. 3A, B).

RNA was isolated from the separated bone and cartilage of the osteochondral biopsies and cartilage-only explants. On the cartilage, qPCR for collagen type 2, aggrecan, collagen type X, *MMP13,* and the aggrecanases *ADAMTS4* and *ADAMTS5* was performed (Fig. 4, $n = 6$). On the bone, qPCR for collagen type 1 was performed (Fig. 3C). *GAPDH* and β-actin were tested as housekeeper genes. Both housekeepers gave comparable results (data not shown); thus, we decided to perform all calculations using the *GAPDH* data. The expression of collagen type 2 and aggrecan decreased over time in biopsy cartilage and for cartilage-only explants, which was more evident for the cartilage-only explants (Fig. 4A). The gene expression of the aggrecanases *ADAMTS4* and *ADAMTS5* remained relatively stable over time in both biopsy cartilage and explants, indicating that our culture conditions did not specifically favored aggrecanase-induced cartilage–ECM deterioration (Fig. 4B). The expression of the hypertrophic markers *MMP13* and collagen type X decreased over time in cartilage from the osteochondral biopsies as well as in

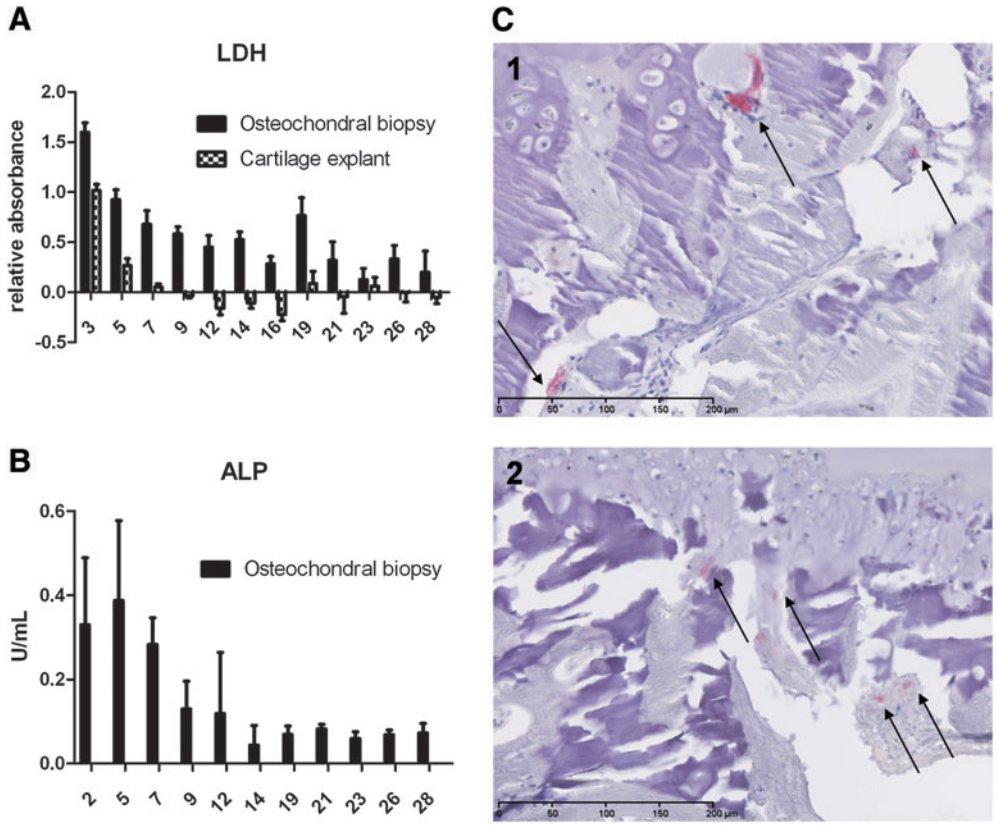

FIG. 2. **(A)** LDH secretion over time detected in medium of osteochondral biopsies and cartilage-only explants; **(B)** ALP activity in time detected in medium of osteochondral biopsies; **(C)** TRAP-stained osteochondral biopsy sections before culture **(C1)** and after 28 days of culture **(C2)**, arrows indicate TRAP-positive cells, scale bars indicate 200 μm. LDH, lactate dehydrogenase; TRAP, tartrate resistant acid phosphatase; ALP, alkaline phosphatase. Color images available online at www.liebertonline.com/tec

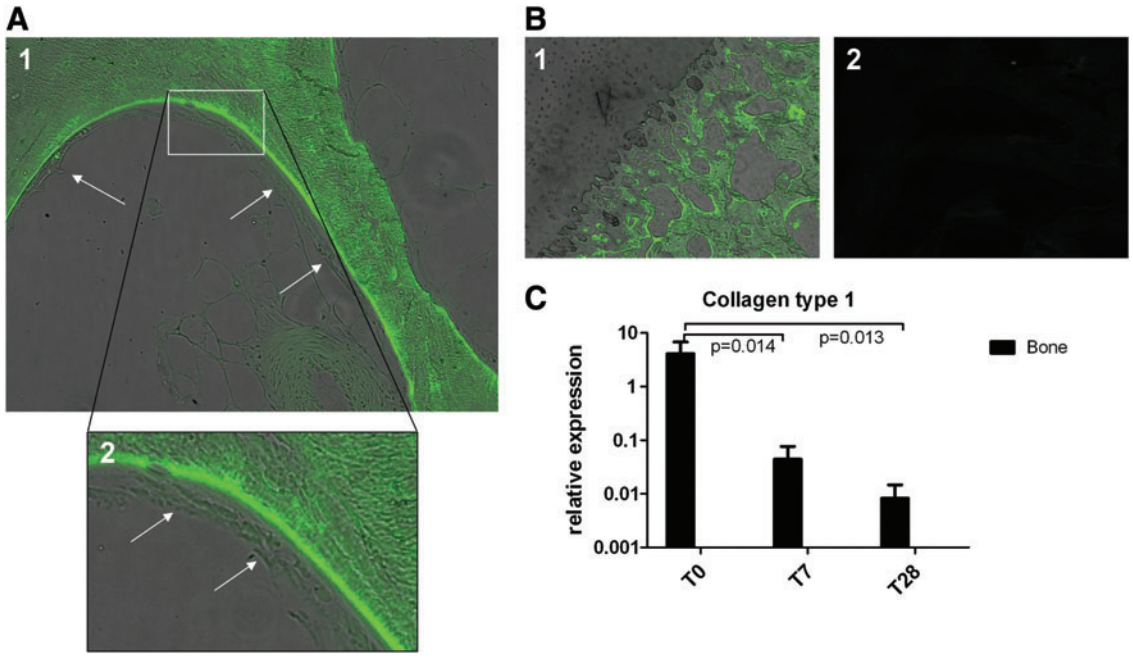

FIG. 3. **(A)** Osteochondral biopsies labeled with calcein after 14 days of culture and harvested after 28 days of culture. Arrows indicate matrix and/or cells deposited during culture after calcein labeling; magnification 20× **(1)** and 40× **(2)**. **(B)** Calcein labeling was specific for bone matrix; (1) Cartilage was not labeled; (2) No autofluorescence of unlabeled osteochondral biopsies was detected; magnification 20×. **(C)** Gene expression of collagen type 1 in bone of the osteochondral biopsies after 0, 7, and 28 days of culture ($n=6$). Color images available online at www.liebertonline.com/tec

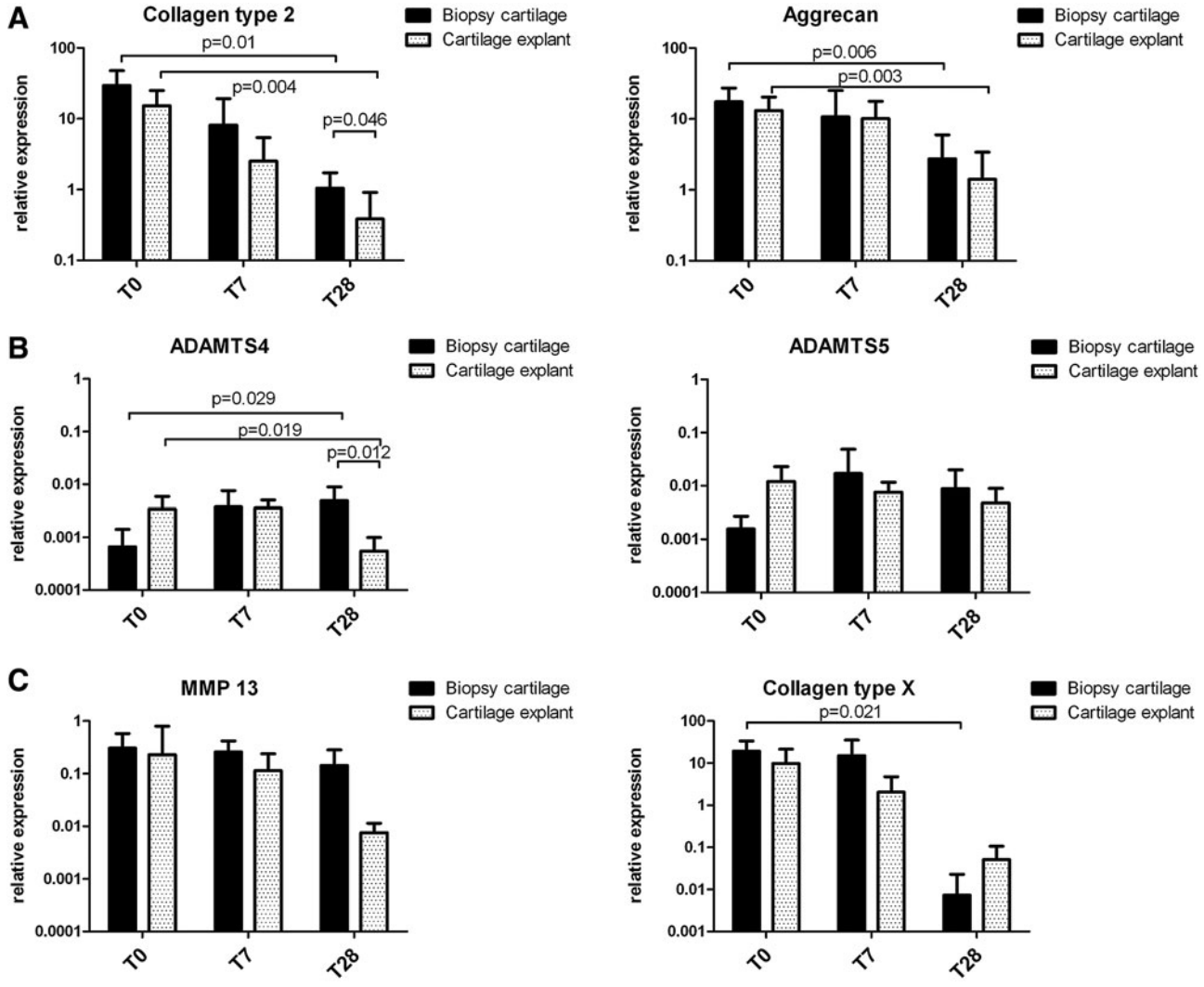

FIG. 4. Mean relative gene expressions ($n=6$) with standard deviations of osteochondral biopsy-cartilage and cartilage-only explants during 28 days of culture. **(A)** The cartilage-related genes collagen type 2 and aggrecan. **(B)** The aggrecanases *ADAMTS4* and *ADAMTS5*. **(C)** The hypertrophy-related genes MMP13 and collagen type X. Gene expressions are calculated relative to *GAPDH*. *MMP13*, matrix metalloproteinase; *ADAMTS*, a disintegrin and metalloproteinase with thrombospondin motifs; *GAPDH*, glyceraldehyde-3-phosphate dehydrogenase.

cartilage-only explants (Fig. 4C). No significant differences were observed in *MMP13* and collagen type X gene expression between osteochondral biopsy cartilage and conventional cartilage explants. This indicates that our culture system did not stimulate hypertrophy. Collagen type 1 expression in osteochondral biopsy bone decreased over time (Fig. 3C).

Testing the applicability of the model for studying cell-based treatments

General morphology of osteochondral biopsies was visualized using H&E staining (Fig. 1D). Defects of three different depths were created successfully and reproducibly (Fig. 5A, $n=9$). Production of glycosaminoglycans, visualized using safranin-O staining, was observed after direct seeding of chondrocytes in defects of different depths and in osteochondral defects with direct-seeded chondrocytes and membrane-seeded chondrocytes. Differences were detected between chondrocyte-seeded defects of different depths in terms of quality and quantity of safranin-O–positive repair tissue (Fig. 5). Significantly more repair tissue was found in osteochondral defects compared with chondral defects (Fig. 5C, $n=9$, $p=0.01$). In terms of integration of newly formed repair tissue, no significant differences were observed between the three different depths of defects (Fig. 5C). Differences were mainly observed in nonquantified terms: the repair tissue is more coherent and more positive for safranin-O for deeper defects (Fig. 5B). Direct seeding of chondrocytes in an osteochondral defect resulted in significantly larger volume of safranin-O–positive tissue as well as a better integration to the bottom of the defect than chondrocytes that were seeded on the membrane before applying in the defect (Fig. 5E).

Discussion

Since multiple mechanisms involved in cartilage repair are still unknown, we believe that a well-characterized *in vitro* model is necessary to elucidate the factors that determine

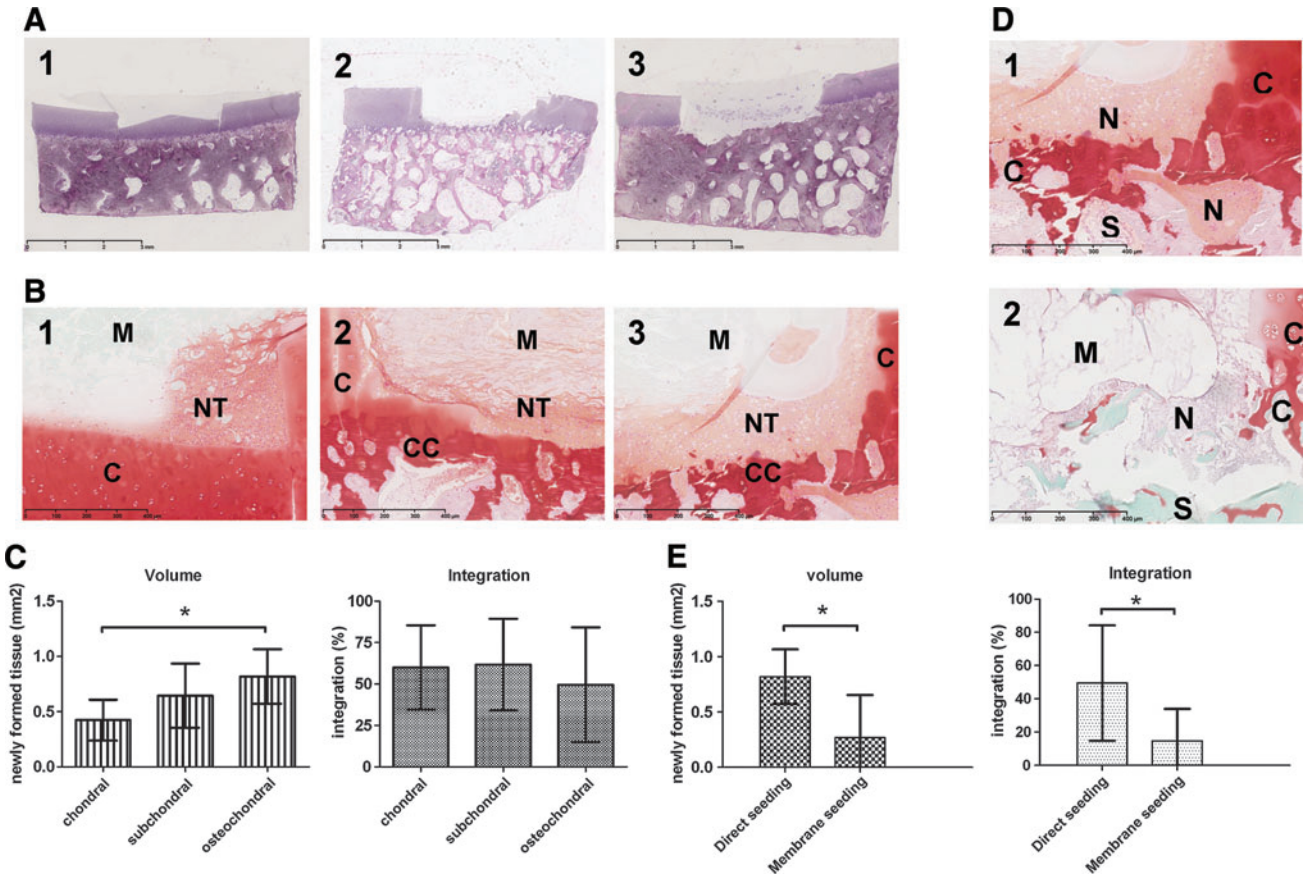

FIG. 5. The two validation settings of the osteochondral culture model. **(A)** Validation setting 1: H&E-stained osteochondral biopsies with defects of chondral **(1)**, subchondral **(2)**, and osteochondral **(3)** depth; scale bars indicate 3 mm. **(B)** Validation setting 1: safranin–O–stained detail images of tissue formed by direct seeded chondrocytes in defects of chondral **(1)**, subchondral **(2)** and osteochondral **(3)** depth; scale bars indicate 400 μm. **(C)** Validation setting 1: scoring of volume and integration of newly formed tissue on safranin-O–stained sections; mean with standard deviation ($n=9$); *indicates $p=0.01$. **(D)** Validation setting 2: direct seeding **(1)** versus membrane seeding **(2)** of bovine chondrocytes in osteochondral defects; scale bars indicate 400 μm. **(E)** Validation setting 2: scoring of volume (*indicates $p=0.01$) and integration (*indicates $p=0.03$) of newly formed tissue on safranin-O–stained sections; mean with standard deviation ($n=9$). NT, newly formed tissue; C, native cartilage; CC, calcified cartilage remains; M, chondrogide membrane. Color images available online at www.liebertonline.com/tec

cartilage repair. We have shown that our osteochondral culture model was viable during 28 days of culture based on three grounds: (1) LDH secretion by the osteochondral biopsies was high shortly after creation of the biopsies but decreased to steady low levels after 7 days; (2) mRNA was retrievable after 28 days in culture; and (3) the subchondral bone was characterized: TRAP-positive cells were present after 28 days in culture, calcein labeling showed matrix deposition, and the ALP assay indicated that the bone was actively remodeling during the culture period. Further, we have demonstrated that different treatments can be evaluated using our model by quantification of the amount of newly formed tissue filling the defect and the integration of this tissue with the defect environment.

The first-described osteochondral models were not intended for *in vitro* use and were directly implanted *in vivo* without *in vitro* characterization.[21,22] We have shown that it was possible to create defects of different depths. Earlier-described models either use one type of defect[23] or do not describe the depth of their defects[24] or do not characterize their model *in vitro*.[21,22] Control over defect depth is of critical importance in modeling and studying cartilage defects and involved repair mechanisms, reflected by the differences we have found in terms of quantity and integration of newly formed repair tissue in defects of different depths. To our knowledge, none of the osteochondral models so far described in literature involved evaluation of the subchondral bone during or after culture. In our model, this was studied by means of TRAP staining, calcein labeling, and ALP activity measurements, which indicated that the subchondral bone remained active during culture.

It is evident that the osteochondral biopsies were not equal after 28 days of culture to the situation before culturing. This is, for example, reflected by the fact that collagen type 2 and aggrecan gene expression in osteochondral biopsy cartilage were lower when cultured for 28 days than it was in native articular cartilage. However, collagen type 2 expression was significantly higher in osteochondral biopsy cartilage than in cartilage-only explants after 28 days of culture, indicating that the osteochondral biopsy provides a more representative culture system. Also, the hypertrophic markers *MMP13* and collagen type X expression decreases over time for both osteochondral biopsy cartilage and cartilage-only explants,

indicating that our culture conditions did not induce hypertrophy of the cultured tissue.

Although our model still differs from the native situation, there are multiple mechanistic factors that make our osteochondral biopsy model more physiologically relevant than the conventional cartilage-only explants due to the presence of the subchondral bone. Subchondral bone and cartilage are closely related anatomically but also influence each other in disease processes.[25–30] Subchondral bone is also identified as a critical success factor of the microfracture procedure.[12,31] These previously reported findings indicate that subchondral bone plays a critical role in repair tissue formation after cartilage repair treatments. The results of gene expression analysis of biopsy-cartilage and cartilage-only explants supported the following result: the presence of subchondral bone resulted in a different expression pattern of cartilage-related genes, supporting that our osteochondral biopsy model is more representative to the native situation than cartilage-only explants.

In vivo cartilage is dependent on diffusion of nutrients and oxygen. Chondrocytes residing in healthy articular cartilage are exposed to a gradient of oxygen and nutrient supply.[32] In cartilage of the osteochondral biopsies, the exposure to oxygen and nutrients of the deep cartilage zone was likely lower than that of the deep zone in cartilage-only explants. In the osteochondral biopsies, nutrients and oxygen need to diffuse through the superficial and middle zone of the cartilage or through the subchondral bone and calcified cartilage to reach the deep-zone cartilage cells. The deep zone of cartilage-only explants is directly exposed to nutrients and oxygen in the culture medium. This makes our osteochondral culture model more similar to the *in vivo* situation than the conventional cartilage-only explant cultures.

Another advantage of the osteochondral model can be that the cartilage is more intact than it is in cartilage-only explants. Cartilage that is explanted or otherwise damaged shows chondrocyte death in wound edges.[33–35] Our osteochondral biopsy model contains not only damage in terms of the created cartilage defects, but also the outer edges of the biopsy itself should be considered as wound area due to the drilling procedure to create the biopsies out of the MCP joints. In the cartilage-only explants, the cartilage wound surface was even relatively larger, since these explants were cut off the subchondral bone, which makes the bottom of the explants a wound surface as well.

A difference between the model and the physiological situation is the absence of mechanical loading during culture. This may be an explanation for the strong decrease observed in the expression of collagen type 1 in the osteochondral biopsy bone. It is well-known that bone is a continuously remodeling tissue that has the capability to respond to the mechanical circumstances it is experiencing: bone needs mechanical stimulation to prevent demineralization and to maintain its mechanical strength.[36] The extension of our model with mechanical loading would provide the opportunity to model healing or regeneration processes of articular cartilage in a more joint-like environment, especially when various mechanical loading patterns can be applied. Further, the presence of synovial fluid in the culture system would also be possible to even better mimic the joint environment. These adaptations to the model can be made in future.

Possible applications of our model are numerous. We have demonstrated two possible approaches: creation of defects of different depths to simulate cartilage damage and two different seeding strategies. Differences were observed in terms of volume and integration of newly formed tissue, indicating that our model can be used to study various cartilage repair mechanisms and features *in vitro*. We observed that the placement of the membrane in the defect was a critical factor for the success of both approaches: if the membrane did not remain in place, poor attachment of seeded cells onto the defect was found, which corresponds with clinical findings—ACI or ACI-derived treatments fail when the periosteal flap or membrane does not stay in place.[37] Cartilage repair treatments could be simulated *in vitro*. ACI and its derivatives could be modeled by applying different cell seeding strategies and membranes to cover the defect or to seed cells on. One could also imagine studying other approaches such as the use of different cell sources and biomaterials for cartilage repair purposes. For example, MSCs, which may provide an attractive cell source for cartilage-regeneration strategies based on their rapid expansion *in vitro* and their chondrogenic differentiation potential.[10,38] Our model could be used, for example, to study the effects of expansion conditions, exposure to growth factors, oxygen tension, or genetic modification of cells by overexpression or knockdown of factors upon or before use on cartilage formation capacity in our model. Another possible application of our model could be the screening and comparison of various biomaterials, for example, for their capacity to fill cartilage defects, to serve as a scaffold for implantation of cells, to study the effect of incorporation of bioactive factors, or to study integration of materials or cells into the defect environment.

Overall, we have developed and validated a reproducible model that can be used in multiple experiments to study many cartilage repair mechanisms *in vitro* both for current treatments of cartilage defects as well as in development of new repair strategies.

Acknowledgment

The research leading to these results has received funding from the Dutch Arthritis Association and the European Union's 7th Framework Programme under grant agreement no. NMP3-SL-2010-245993.

Disclosure Statement

The authors state that no competing financial interests exist.

References

1. Brittberg, M., *et al.* Treatment of deep cartilage defects in the knee with autologous chondrocyte transplantation. N Engl J Med **331,** 889, 1994.
2. Shah, M.R., *et al.* Articular cartilage restoration of the knee. Bull NYU Hosp Jt Dis **65,** 51, 2007.
3. Marlovits, S., *et al.* Cartilage repair: generations of autologous chondrocyte transplantation. Eur J Radiol **57,** 24, 2006.
4. Steadman, J.R., *et al.* Microfracture technique for full-thickness chondral defects: technique and clinical results. Op Tech Orthop **7,** 300, 1997.
5. Steadman, J.R., *et al.* [The microfracture technic in the management of complete cartilage defects in the knee joint].

Die Technik der Mikrofrakturierung zur Behandlung von kompletten Knorpeldefekten im Kniegelenk. Orthopade **28,** 26, 1999.
6. Steinwachs, M.R., Guggi, T., and Kreuz, P.C. Marrow stimulation techniques. Injury **39 Suppl 1,** S26, 2008.
7. Knutsen, G., *et al.* Autologous chondrocyte implantation compared with microfracture in the knee. A randomized trial. J Bone Joint Surg Am **86A,** 455, 2004.
8. Moseley, J.B., Jr., *et al.* Long-term durability of autologous chondrocyte implantation: a multicenter, observational study in US patients. Am J Sports Med **38,** 238, 2010.
9. Peterson, L., *et al.* Autologous chondrocyte transplantation. Biomechanics and long-term durability. Am J Sports Med **30,** 2, 2002.
10. Bos, P.K., van Melle, M.L., and van Osch, G.J.V.M. Articular cartilage repair and the evolving role of regenerative medicine. Open Access Surg **3,** 109, 2010.
11. van Osch, G.J., *et al.* Cartilage repair: past and future—lessons for regenerative medicine. J Cell Mol Med **13,** 792, 2009.
12. Frisbie, D.D., *et al.* Effects of calcified cartilage on healing of chondral defects treated with microfracture in horses. Am J Sports Med **34,** 1824, 2006.
13. Frisbie, D.D. A comparative study of articular cartilage thickness in the stifle of animal species used in human pre-clinical studies compared to articular cartilage thickness in the human knee. Vet Comp Orthop Traumatol **19,** 142, 2006.
14. Mithoefer, K., *et al.* Clinical efficacy of the microfracture technique for articular cartilage repair in the knee: an evidence-based systematic analysis. Am J Sports Med **37,** 2053, 2009.
15. Lowry, O.H., *et al.* The quantitative histochemistry of brain. II. Enzyme measurements. J Biol Chem **207,** 19, 1954.
16. Erlebacher, A., and Derynck, R. Increased expression of TGF-beta 2 in osteoblasts results in an osteoporosis-like phenotype. J Cell Biol **132,** 195, 1996.
17. Scheven, B.A., *et al.* Differentiation kinetics of osteoclasts in the periosteum of embryonic bones in vivo and in vitro. Anat Rec **214,** 418, 1986.
18. Sniekers, Y.H., *et al.* Estrogen modulates iodoacetate-induced gene expression in bovine cartilage explants. J Orthop Res **28,** 607, 2010.
19. Jenniskens, Y.M., *et al.* Biochemical and functional modulation of the cartilage collagen network by IGF1, TGFbeta2 and FGF2. Osteoarthritis Cartilage **14,** 1136, 2006.
20. Livak, K.J., and Schmittgen, T.D. Analysis of relative gene expression data using real-time quantitative PCR and the 2(-Delta Delta C(T)) method. Methods **25,** 402, 2001.
21. Mueller-Rath, R., *et al.* In vivo cultivation of human articular chondrocytes in a nude mouse-based contained defect organ culture model. Biomed Mater Eng **17,** 357, 2007.
22. Schuller, G.C., *et al.* An in vivo mouse model for human cartilage regeneration. J Tissue Eng Regen Med **2,** 202, 2008.
23. Iwai, R., *et al.* Ex vivo cartilage defect model for the evaluation of cartilage regeneration using mesenchymal stem cells. J Biosci Bioeng **111,** 357, 2011.
24. Secretan, C., Bagnall, K.M., and Jomha, N.M. Effects of introducing cultured human chondrocytes into a human articular cartilage explant model. Cell Tissue Res **339,** 421, 2010.
25. Botter, S.M., *et al.* Cartilage damage pattern in relation to subchondral plate thickness in a collagenase-induced model of osteoarthritis. Osteoarthritis Cartilage **16,** 506, 2008.
26. Botter, S.M., *et al.* ADAMTS5-/- mice have less subchondral bone changes after induction of osteoarthritis through surgical instability: implications for a link between cartilage and subchondral bone changes. Osteoarthritis Cartilage **17,** 636, 2009.
27. Sniekers, Y.H., *et al.* Oestrogen is important for maintenance of cartilage and subchondral bone in a murine model of knee osteoarthritis. Arthritis Res Ther **12,** R182, 2010.
28. Sniekers, Y.H., *et al.* Development of osteoarthritic features in estrogen receptor knockout mice. Osteoarthritis Cartilage **17,** 1356, 2009.
29. Intema, F., *et al.* Subchondral bone remodeling is related to clinical improvement after joint distraction in the treatment of ankle osteoarthritis. Osteoarthritis Cartilage **19,** 668, 2011.
30. Zhang, L., *et al.* Enhancement of subchondral bone quality by alendronate administration for the reduction of cartilage degeneration in the early phase of experimental osteoarthritis. Clin Exp Med 2011 [Epub ahead of print; DOI: 10-1007/s10238-011-0131-z].
31. Frisbie, D.D., *et al.* Early events in cartilage repair after subchondral bone microfracture. Clin Orthop Relat Res **407,** 215, 2003.
32. Pfander, D., and Gelse, K. Hypoxia and osteoarthritis: how chondrocytes survive hypoxic environments. Curr Opin Rheumatol **19,** 457, 2007.
33. Bos, P.K., *et al.* Growth factor expression in cartilage wound healing: temporal and spatial immunolocalization in a rabbit auricular cartilage wound model. Osteoarthritis Cartilage **9,** 382, 2001.
34. Bos, P.K., Verhaar, J.A., and van Osch, G.J. Age-related differences in articular cartilage wound healing: a potential role for transforming growth factor beta1 in adult cartilage repair. Adv Exp Med Biol **585,** 297, 2006.
35. Tew, S.R., *et al.* The reactions of articular cartilage to experimental wounding: role of apoptosis. Arthritis Rheum **43,** 215, 2000.
36. Wolff, J. The law of bone remodeling translation of the german 1892 version. Berlin: Springer, 1986.
37. Niemeyer, P., *et al.* Characteristic complications after autologous chondrocyte implantation for cartilage defects of the knee joint. Am J Sports Med **36,** 2091, 2008.
38. Johnstone, B., *et al.* In vitro chondrogenesis of bone marrow-derived mesenchymal progenitor cells. Exp Cell Res **238,** 265, 1998.

Address correspondence to:
Gerjo J.V.M. van Osch, Ph.D.
Department of Orthopaedics and Otorhinolaryngology
Erasmus MC
University Medical Centre Rotterdam
P.O. Box 2040
Rotterdam, 3000 CA
The Netherlands

E-mail: g.vanosch@erasmusmc.nl

Received: June 16, 2011
Accepted: August 29, 2011
Online Publication Date: October 17, 2011